Improvement of load-following capacity of grate boilers based on the combustion power soft-sensor

Jukka Kortela
Aalto University School of Chemical Technology
PL 16100, FI-00076 Aalto
Email: jukka.kortela@aalto.fi

Sirkka-Liisa Jämsä-Jounela
Aalto University School of Chemical Technology
PL 16100, FI-00076 Aalto
Email: sirkka-liisa.jamsa-jounela@aalto.fi

***Abstract*—For improving the load-following capacity of existing grate boiler units, an MPC control concept based on the combustion power soft-sensor is developed. Because the combustion power estimation has a very quick response to the primary air flow input, the load-following speed of the boiler control system will be improved considerably. The proposed MPC strategy is tested with the BioPower 5 CHP plant data and the results are presented, analyzed, and discussed.**

I. Introduction

Renewable energy sources are considered on the priority level of energy policies in Europe and many other contries worldwide. The European commission has endorsed a mandatory target of a 20 % share of energy from renewable sources in overall consumption by 2020. This leads to an introduction of an increasing share of energy produced from natural resources, such as hydro power, wind, solar, wave, geothermal, waste fuels, as well as biomass and waste heat, in to the existing energy networks. With more and more wind power and solar power units integration on power systems, there has been an increased demand on the load-following capabilities of the other power units.

In [1], Wang et al. proposed an improved coordinated control strategy (CCS) combined with cold flow adjustment on account that cold source parameter has rapid and large influence on the turbine power output. The control strategy utilizes CSFA (cold source flow adjustment) to accelerate the load following capability, coal feeder rate to ensure the control accuracy of turbine load, and the turbine governor valve to avoid large fluctuation of main steam pressure. The simulation studies on the 300 MW unit showed that after 10 MW step order of turbine power is given, the turbine power with improved strategy reached its equilibrium state after about 7 seconds. However, it took over 50 seconds when using the traditional CSS. In addition, the improved strategy had a much smaller overshoot that traditional CSS.

Mortensen et al. [2] developed a control concept based on a scheduled LQG controller with coordinated feedforward from the boiler load demand to fuel flow and feedwater flow for the purpose of improving the load-following capability of existing power-plant units. Field tests on the 265 MW coal-fired power plant unit revealed that the maximum allowable load gradient can be increased from 4 to 8 MW/min without further plant stress.

Wang et al. [3] a new method for the boiler control system based on radiation intensity for improving the load-following capacity of a coal-fired power plant. Field tests on a 300 MW coal-fired plant revealed that the improved boiler control system increased the load-following capacity. Also, indirect methods have been used to measure radiation intensity or combustion power in the furnace. According to [4], the theoretical studies and practical tests at the coal power plant the fuel combustion power can be estimated on the basis of the measured oxygen consumption. The method assumed a constant fuel moisture content, although the relative ration of oxygen in flue gas is affected by the variation of the fuel moisture content, which introduces the error to the estimation.

Recently, the above mentioned combustion power method was improved by Kortela and Jämsä-Jounela [5] who estimated the fuel moisture content from the dynamic energy balance of the secondary superheater involving the combustion power estimation. Because the combustion power estimation has a very quick response of less than 1.5 minutes to the primary air flow input, the load-following speed of the boiler control system will be improved considerably.

In this paper an improvement of load-following capacity of BioPower 5 CHP plant is presented. The paper is organized as follows: Section 2 presents the BioPower 5 CHP process. The developed MPC strategy is presented in Section 3. The test results are given in Section 4, followed by the conclusions in Section 5.

II. Description of the BioPower 5 CHP process

The BioPower 5 CHP process consists of two main parts: the furnace and the steam-water circuit. The heat used for steam generation is obtained by burning solid biomass fuel – consisting of bark, sawdust, and pellets – which is fed into the furnace together with combustion air. The heat of the flue gas is transfered by the heat exchangers to the steam-water circulation, where superheated steam is generated [6].

In the BioGrate system, the fuel is fed onto the center of a grate from below through a stoker screw, as shown in Fig. 1. The grate consists of alternate rotating and stationary concentric rings with the rotating rings alternately rotated clockwise and counter-clockwise by hydraulics. This design distributes the fuel evenly over the entire grate, with the burning fuel forming an even layer of the required thickness.

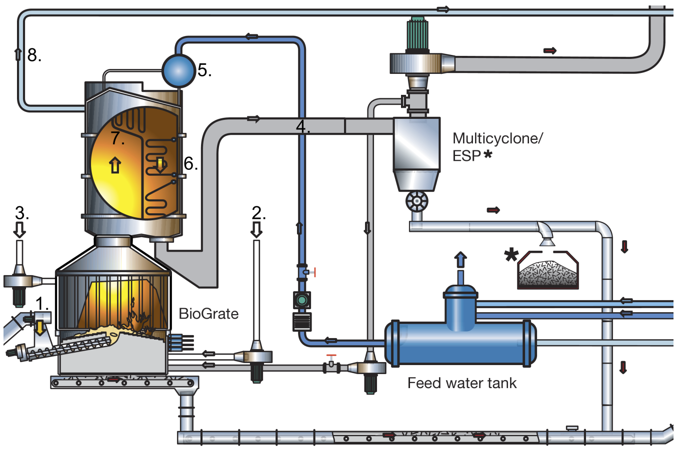

Fig. 1. 1. Fuel, 2. Primary air, 3. Secondary air, 4. Economizer, 5. Drum, 6. Evaporator, 7. Superheaters, 8. Superheated steam

The moisture content of the wet fuel in the centre of the grate evaporates rapidly due to the heat of the surrounding burning fuel and the thermal radiation coming from the brick walls. The gasification and visible combustion of the gases and solid carbon takes place as the fuel moves to the periphery of the circular grate. At the edge of the grate, ash finally falls into a water-filled ash basin underneath the grate.

The primary air for combustion and the recirculation flue gas are fed from underneath the grate and they penetrate the fuel through the slots in the concentric rings. The secondary air is fed directly into the flame above the grate and the air distribution is controlled by dampers and speed-controlled fans. The gases released from biomass conversion on the grate and a small number of entrained fuel particles continue to combust in the freeboard, in which the secondary air supply plays a significant role in the mixing, burnout, and the formation of emissions. The design of the air supply system, the ratio between primary and secondary air, plays a key role in the efficient and complete combustion of biomass [7]. In modern grate-fired boilers burning biomass, the split ratio of primary to secondary air is 40/60, which should be followed by a control design for the most efficient energy production. The overall excess air for most biomass fuels is normally set at 25% or above.

The essential components of the water-steam circuit are an economizer, a drum, an evaporator, and superheaters. Feed water is pumped from a feed water tank into the boiler. First the water is led into the economizer (4), which is the last heat exchanger extracting the energy from the flue gas, and thus, improving the efficiency of the boiler. From the economizer, the heated feed water is transferred into the drum (5) and along downcomers into the bottom of the evaporator (6) through tubes that surround the boiler. From the evaporator tubes, the heated water and steam return back into the steam drum, where they are separated. The steam rises to the top of the steam drum and flows into the superheaters (7) where it heats up further and superheats. The superheated high-pressure steam (8) is then passed into the steam turbine, where electricity is generated.

A. Model Description of the BioGrate Boiler

The set of mathematical equations describing the process is given as,

$$
\begin{aligned}
\dot{x}_1(t) &= c_{ds}x_1(t) - c_{thd}\beta_{thd}u_2(t) + c_{ds,in}u_1(t), && (1)\\
\dot{x}_2(t) &= -c_{wev}\beta_{wev}x_2(t) + c_{w,in}d_1(t), && (2)\\
\dot{x}_3(t) &= -x_3(t) + q_{wf}(c_{thd}\beta_{thd}u_2(t) - c_{ds}x_1(t)) && (3)\\
&\quad -0.0244c_{wev}\beta_{wev}x_2(t), && (4)\\
\dot{x}_4(t) &= -x_4(t) + d_2(t), && (5)\\
\dot{x}_5(t) &= \frac{1}{\alpha_{metal}}(x_3(t) - x_4(t)), && (6)\\
\dot{x}_6(t) &= -x_6(t) + c_{ds,O_2}x_1(t) + c_{wev,O_2}x_2(t) && (7)\\
&\quad +c_{thd,O_2}u_2(t) + c_{ds,in,O_2}u_1(t), && (8)
\end{aligned}
$$

where $x_1(t)$, $x_2(t)$, $x_3(t)$, $x_4(t)$, $x_5(t)$ and $x_6(t)$ are the fuel bed height, the moisture content in the furnace, the power generated from the biomass combustion, the filtered steam demand, the drum pressure and the oxygen content in flue gas respectively; $u_1(t)$, $u_2(t)$ and $u_3(t)$ are the fuel flow rate, the primary air flow rate and the secondary air flow rate respectively; $d_1(t)$ and $d_2(t)$ are measured disturbances and consist of the moisture content in the fuel and the steam demand respectively; c_{ds}, c_{thd}, $c_{ds,in}$, c_{wev} and $c_{w,in}$ are model coefficients identified from process data; β_{thd} describes the dependence on the position of the moving grate; β_{wev} is the coefficient for a dependence on the position from the centre to the periphery of the moving grate; α_{metal} is a coefficient that depends on the material type of the metal tubes of the evaporator system; c_{ds,O_2}, c_{wev,O_2}, c_{thd,O_2} and c_{ds,in,O_2} are the parameters for the linearized model of the oxygen content.

III. Model predictive control for the BioGrate boiler

The objective of the MPC strategy is to improve the load-following capabilty of existing grate boilers. The MPC configuration is as follows: the primary air flow rate and the stoker speed are the manipulated variables (u); the moisture content in the fuel feed and the steam demand are the measured disturbances (d); and the fuel bed height, the combustion power, and the steam pressure are the controlled variables (y). The MPC scheme is presented in Fig. 2. The combustion power and fuel moisture soft-sensors are used to compensate the effect of the fuel quality variations. The results show that these soft-sensors predict the thermal decomposition rate of dry fuel and the water evaporation with good precision. Furthermore, the results of the tests show that these methods are able to detect variations in these properties within seconds [5]. In particular, the fuel moisture estimation is considered by the MPC as a measured disturbance and is also used to estimate the amount of water in the furnace. Considering the combustion power as a model state improves the load-following capabilty of the boiler during the transitions. In addition, the thermal decomposition rate is used in the calculations of the fuel bed height. In order

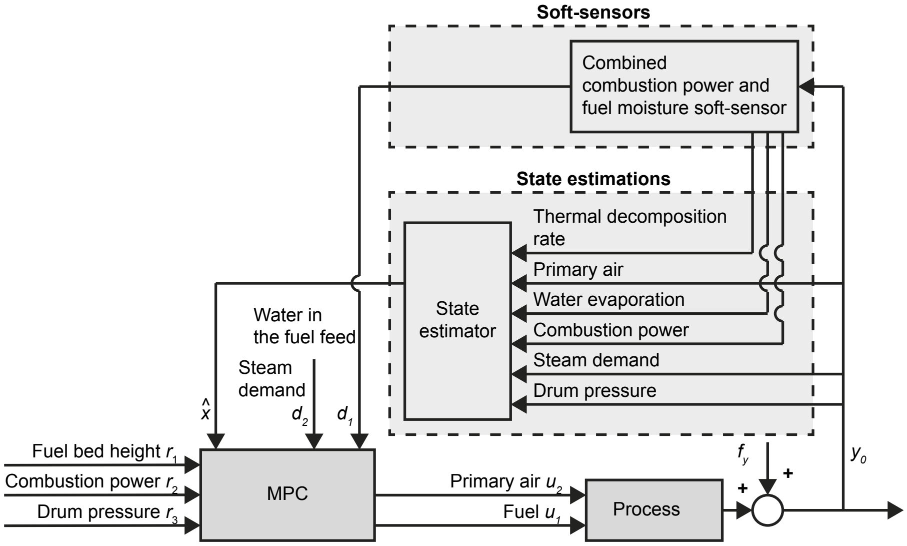

Fig. 2. MPC of the BioGrate boiler

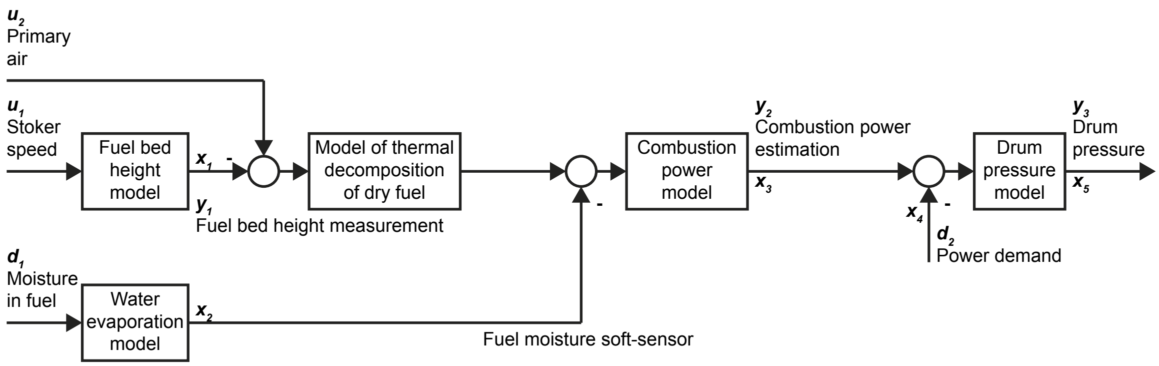

Fig. 3. The models of the BioGrate boiler

to design the MPC a sample data model of the process has been obtained by zero-order hold discretization with sampling time $T_s = 1\,\mathrm{s}$. Hence, from now on, we will refer to the following discrete-time

$$\begin{aligned} x(k+1) &= Ax(k) + Bu(k) + Ed(k), \\ y(k) &= Cx(k). \end{aligned} \tag{9}$$

According to (9), the k-step ahead prediction is formulated as:

$$y(k) = CA^k x(0) + \sum_{j=0}^{k-1} H(k-j)u(j) \tag{10}$$

where $H(k-j)$ contains the impulse response coefficients. Therefore, using (10), the MPC optimization problem consists in minimizing

$$\phi = \frac{1}{2}\sum_{k=1}^{N_p} \|y(k) - r(k)\|^2_{Q_z} + \frac{1}{2}\|\Delta u(k)\|^2_{Q_u} \tag{11}$$

under the constraints

$$\begin{aligned} x(k+1) &= Ax(k) + Bu(k) + Ed(k), \quad k = 0, 1, \ldots, N_p - 1, \\ y(k) &= Cx(k), \quad k = 0, 1, \ldots, N_p, \\ u_{\min} &\le u(k) \le u_{\max}, \quad k = 0, 1, \ldots, N_p - 1, \\ \Delta u_{\min} &\le \Delta u(k) \le \Delta u_{\max}, \quad k = 0, 1, \ldots, N_p - 1, \\ y_{\min} &\le y(k) \le y_{\max}, \quad k = 1, 2, \ldots, N_p, \end{aligned}$$

where $r(k)$ is the target value and $\Delta u(k) = u(k) - u(k-1)$. The predictions by (10) are formulated as presented in [8] and the MPC regulator problem of (11) is then solved by convex quadric programming algorithms.

The original system (9) is augmented with disturbance dynamics to achieve the offset-free tracking in the presence of model-plant mismatch or unmeasured disturbances [9]. Hence, the extended system is the following

$$\begin{bmatrix} x(k+1) \\ \eta(k+1) \end{bmatrix} = \begin{bmatrix} A & B_d \\ 0 & A_d \end{bmatrix} \begin{bmatrix} x(k) \\ \eta(k) \end{bmatrix} + \begin{bmatrix} B \\ 0 \end{bmatrix} u(k) \tag{12}$$

$$+ \begin{bmatrix} E \\ 0 \end{bmatrix} d(k) + \begin{bmatrix} w(k) \\ \xi(k) \end{bmatrix}, \tag{13}$$

$$y(k) = \begin{bmatrix} C & C_\eta \end{bmatrix} \begin{bmatrix} x(k) \\ \eta(k) \end{bmatrix} + v(k), \tag{14}$$

where $w(k)$ and $v(k)$ are white noise disturbances with zero mean. Thus, the disturbances and the states of the system are estimated as follows:

$$\begin{bmatrix} \hat{x}(k|k) \\ \hat{\eta}(k|k) \end{bmatrix} = \begin{bmatrix} \hat{x}(k|k-1) \\ \hat{\eta}(k|k-1) \end{bmatrix}$$

$$+ \begin{bmatrix} L_x \\ L_\eta \end{bmatrix} (y(k) - C\hat{x}(k|k-1) - C_\eta \hat{\eta}(k|k-1)) \tag{15}$$

and the state predictions of the augmented system (12) are obtained by:

$$\begin{bmatrix} \hat{x}(k+1|k) \\ \hat{\eta}(k+1|k) \end{bmatrix} = \begin{bmatrix} A & B_d \\ 0 & A_d \end{bmatrix} \begin{bmatrix} \hat{x}(k|k) \\ \hat{\eta}(k|k) \end{bmatrix}$$

$$+ \begin{bmatrix} B \\ 0 \end{bmatrix} u(k) + \begin{bmatrix} E \\ 0 \end{bmatrix} d(k). \tag{16}$$

Additional disturbances, $\eta(k)$, are not controllable by the inputs u. However, since they are observable, their estimates are used to remove their influence from the controlled variables. The disturbance model is defined by choosing the matrices B_d and C_η. Since the additional disturbance modes introduced by disturbance are unstable, it is necessary to check the detectability of the augmented system. The augmented system (12) is detectable if and only if the nonaugmented system (9) is detectable, and the following condition holds:

$$\operatorname{rank} \begin{bmatrix} I - A & -B_d \\ C & C_\eta \end{bmatrix} = n + n_\eta, \tag{17}$$

where n_η is the dimension of A_d. In addition, if the system is augmented with a number of integrating disturbances n_η equal to the number of the measurements p ($n_\eta = p$) and if the closed-loop system is stable and constraints are not active at a steady state, there is zero offset in controlled variables.

IV. Test results of the load-following capacity of the MPC strategy

A. Description of the simulation and testing environment

To test the load-following capacity of the developed MPC strategy, a simulation model of the BioPower 5 CHP plant was build and the code for the MPC was developed in MATLAB environment. Parameters of the models of the water evaporation, the thermal decomposition of the dry fuel, and the drum were identified by using the data from the BioPower 5 CHP plant.

B. Test results of the load-following capacity of the MPC strategy

The developed MPC strategy was compared with the conventional MPC strategy where the heat signal as a feedback signal is determined only by the steam pressure and the steam flow.

The input limits were $u_{1,min} = 0$, $u_{1,max} = 4$, $\Delta u_{1,min} = -0.03$, and $\Delta u_{1,max} = 0.03$ [kg/s] for the stoker speed; $u_{2,min} = 0$, $u_{2,max} = 4$, $\Delta u_{2,min} = -0.03$, and $\Delta u_{2,max} = 0.03$ [kg/s] for the primary air.

In the developed MPC strategy, the output limits were $y_{1,min} = 0.2$, $y_{1,max} = 1$ [m] for the fuel bed height; $y_{2,min} = 0$, $y_{2,max} = 30$ [MW] for the combustion power; and $y_{2,min} = 0$, $y_{2,max} = 55$ [bar] for the drum pressure.

$$\mathbf{Q}_{z,1} = \begin{bmatrix} 0.001 & 0 & 0 \\ 0 & 0.001 & 0 \\ 0 & 0 & 0.1 \end{bmatrix} \quad \text{and} \quad \mathbf{Q}_{u,1} = \begin{bmatrix} 0.1 & 0 \\ 0 & 0.1 \end{bmatrix}$$

In the conventional MPC strategy, the output limits was $y_{3,min} = 0$, $y_{3,max} = 55$ [bar] for the drum pressure.

$$\mathbf{Q}_{z,2} = \begin{bmatrix} 0.1 \end{bmatrix} \quad \text{and} \quad \mathbf{Q}_{u,2} = \begin{bmatrix} 0.1 & 0 \\ 0 & 0.1 \end{bmatrix}$$

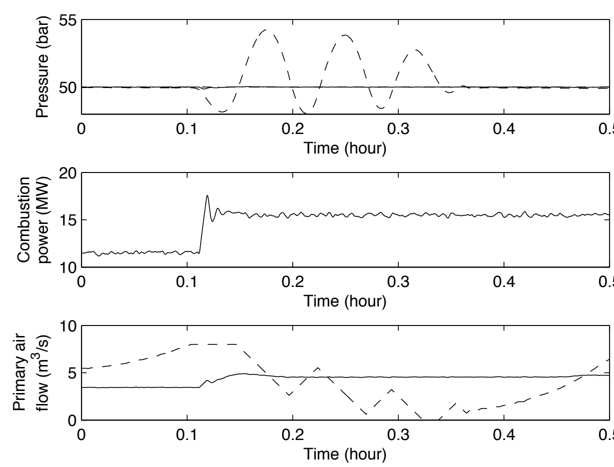

Fig. 4. The improved MPC control strategy (solid line) and the conventional control strategy (dashed line) responses for the change in steam demand

In the simulation test, the steam demand was changed from 12 MW to 16 MW while the moisture content in the fuel feed was kept at 57 %. From the simulation curves Figs. 4-5 it can been seen that change in the steam demand had almost no effect on the drum pressure. However, it would take almost half an hour to make a new balance at 16 MW when using the conventional control strategy.

V. Conclusion

For improving the load-following capacity of existing grate boiler units, an MPC control concept based on the combustion

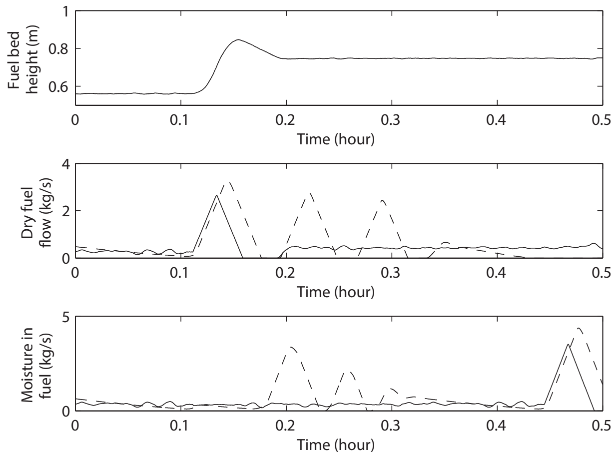

Fig. 5. The improved MPC control strategy (solid line) and the conventional control strategy (dashed line) responses for the change in steam demand

power soft-sensor was developed. Based on the simulation results, significant improvements in the control of critical process variables were obtained during load changes. Due to the general applicability of the method, it could be used for similar processes and thus the same advantages could be achieved in other plants regardless of the fuels and burning methods used.

REFERENCES

[1] W. Wang, J. Liu, D. Zeng, Y. Niu and C. Cui (2015). An improved coordinated control strategy for boiler-turbine units supplemented by cold source flow adjustment. *Energy*, 88, 927 – 934.

[2] J. H. Mortensen, T. Moelbak, P. Andersen, T. S. Pedersen (1998). Optimization of boiler control to improve the load-following capability of power-plant units. *Control Engineering Practice*, 6, 1531 – 1539.

[3] F. Wang, Q. Huang, D. Liu, J. Yan, and K. Cen (2008). Improvement of Load-Following Capacity Based on the Flame Radiation Intensity Signal in a Power Plant. *Energy & Fuels*, 22, 1731 – 1738.

[4] U. Kortela and P. Lautala (1982). A new control concept for a coal power plant. *Control Science and Technology for the Progress of Society*, 6, 3017 – 3023.

[5] J Kortela, S-L Jämsä-Jounela (2013). Fuel moisture soft-sensor and its validation for the industrial BioPower 5 CHP plant. *Applied Energy*, 105, 66–74.

[6] A Boriouchkine, A Zakharov, and S-L Jämsä-Jounela (2012). Dynamic modeling of combustion in a BioGrate furnace: The effect of operation parameters on biomass firing. *Chemical Engineering Science*, 69(1), 669–678.

[7] C Yin, L. A. Rosendahl,, and S. K. Kær, (2008). Grate-firing of biomass for heat and power production. *Progress in Energy and Combustion Science*, 34(6), 725–754.

[8] J Kortela, S-L Jämsä-Jounela (2015). Modeling and model predictive control of the BioPower combined heat and power (CHP) plant. *International Journal of Electrical Power & Energy Systems*, 65, 453–462.

[9] G Pannocchia, J. B. Rawlings (2003). Disturbance Models for Offset-Free Model-Predictive Control *AIchE Journal*, 49 (2), 426–437.